European Journal of Medicinal Chemistry 46 (2011) 58–64

Contents lists available at ScienceDirect

European Journal of Medicinal Chemistry

journal homepage: http://www.elsevier.com/locate/ejmech

Original article

Self-organizing molecular field analysis on human β-secretase nonpeptide inhibitors: 5, 5-disubstituted aminohydantoins

Zhi Li [a,1], Meng Zhou [a], Feng Wu [a], Rui Li [a,b,*,1], Zhenyu Ding [a]

[a] State Key Laboratory of Biotherapy and Cancer Center, West China Hospital, Sichuan University, Chengdu, 610041 Sichuan, PR China
[b] State Key Laboratory of Drug Research, Shanghai Institute of Materia Medica, Chinese Academy of Sciences, 201203 Shanghai, PR China

ARTICLE INFO

Article history:
Received 18 June 2010
Received in revised form
12 October 2010
Accepted 14 October 2010
Available online 19 November 2010

Keywords:
BACE-1
3D-QSAR
SOMFA
Aminohydantoins
Autodock4

ABSTRACT

5, 5-disubstituted aminohydantoins have been recently reported as potent and selective human β-secretase (BACE-1) inhibitors. Self-Organizing Molecular Field Analysis (SOMFA) is used to study the correlation between the molecular properties and biological activities of the 5, 5-disubstituted aminohydantoins inhibitors. Four different alignments and two charge-assigning methods were investigated. The model derived from the superposition of docked conformation with AM1 charge showed satisfied predictive ability, which has good non-cross-validated r^2 (0.842), cross-validated q^2 (0.792), F-test value (254.75) and satisfied predictive ability r^2_{pred} (0.721). Analysis of SOMFA model may provide some useful information in the design of BACE-1 inhibitors with better spectrum of activity.

1. Introduction

Alzheimer's disease (AD) is a common and serious disease among the elderly all over the world, which is characterized by loss of memory and cognition [1]. The significant pathological feature is the extracellular insoluble amyloid senile plaques and intracellular neurofibrillary tangles [2]. The predominant chemical composition amyloid beta peptide (Aβ), a 40 to 42 amino acid peptide, is generated by the proteolysis of β-amyloid precursor protein (APP) in the presence of β-secretase (BACE-1) and γ-secretase [3]. According to a recent study, the proteolysis mediated by β-secretase is considered as a rate-limiting step in the whole proteolytic process. BACE-1 knock out mice display a sharp decline of Aβ production and a normal phenotype [4]. Hence, BACE-1 is a prospective drug design target in the treatment of AD.

BACE-1 is an important member of aspartyl protease family [5]. Research about the inhibitor of aspartate protease becomes a hotspot in some serious diseases, such as HIV and renin pathology. In this respect, in recent years, a variety of excellent BACE-1 inhibitors have been designed. Most of them show a peptide like structure and replacement of cleavable amide bond by a noncleavable transition state isostere [6]. Despite of the excellent low nanomolar inhibitory potency for BACE-1, these compounds have fatal weaknesses in the pharmaceutical characteristics such as low oral bioavailability, poor blood brain barrier permeability, and susceptibility to P-glycoprotein transport, caused by the peptide like structure. Considering the insuperable difficulty of peptide inhibitor, many groups focus their attention on a small molecule nonpeptide BACE-1 inhibitor with the expectation of obtaining a kind of successful inhibitors with both high potency and good pharmaceutical characteristics [7]. Based on this idea, many novel nonpeptide BACE-1 inhibitors are invented in the past five years, such as 1, 3, 5-trisubstituted aromatic derivatives [8], 5, 5-disubstituted aminohydantoin derivatives [9], isophthalamide derivatives [10], 2-amino-thiazole derivatives [11], 2-amino-pyridine derivatives [12], 2-amino-quinazoline derivatives [13], acylguanidine derivatives [14], piperazine derivatives [15] and so on. (Fig. 1)

The self-organizing molecular field analysis (SOMFA) [16] is a simple three-dimensional quantitative structure-activity relationship (3D-QSAR) technique similar to comparative molecular field analysis (CoMFA) [17]. The method uses a grid-based approach without evaluation of probe interaction energies. The molecular shape and electrostatic potential are used to develop the QSAR models. The purpose of this paper is to describe the application of self-organizing molecular field analysis, SOMFA, on a series of 5, 5-disubstituted aminohydantoins (Table 1) to investigate optimal

* Corresponding author. No.1, Keyuan Road 4, Gaopengdadao, Gaoxin District, Chengdu, PR China. Tel.: +86 28 85164063; fax: +86 28 85164060.
E-mail address: lirui@scu.edu.cn (R. Li).
[1] Zhi Li and Rui Li equally contributed to this paper.

0223-5234/$ – see front matter © 2010 Elsevier Masson SAS. All rights reserved.
doi:10.1016/j.ejmech.2010.10.014

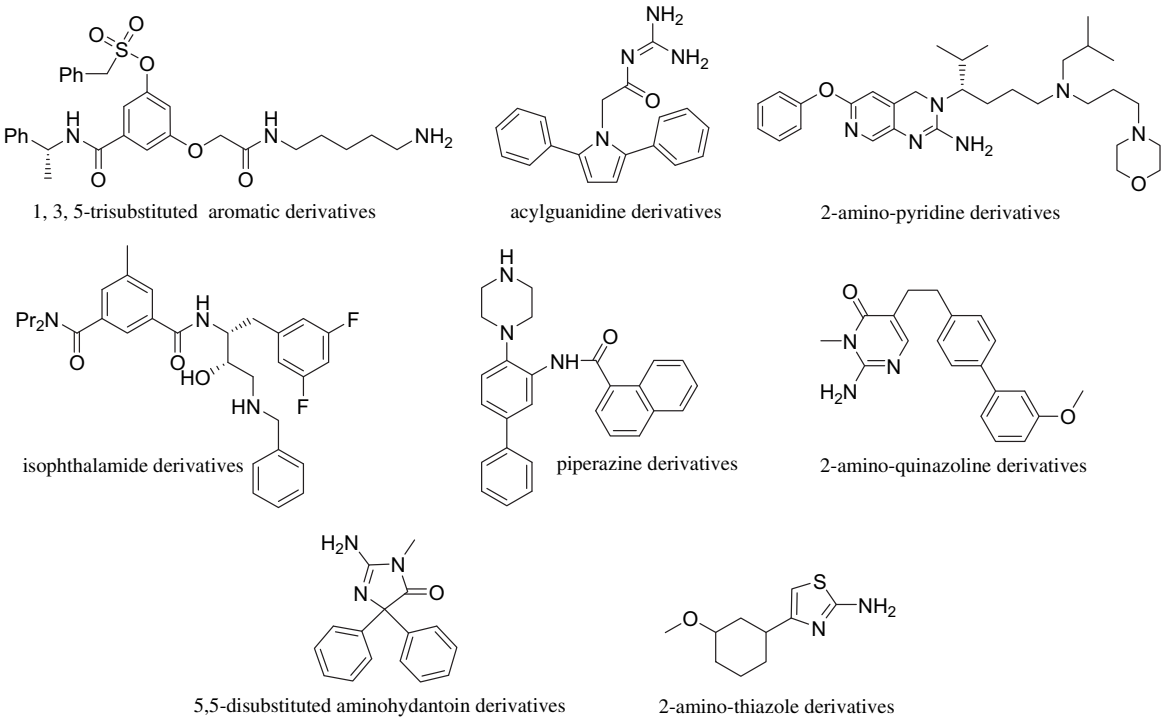

Fig. 1. BACE-1 nonpeptide inhibitors [8–15].

Table 1
Actual and SOMFA predicted pIC_{50} of training and test set for 5, 5-disubstituted aminohydantoins.

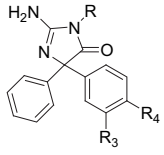

Compound	R	R_3	R_4	Observed	Predicted	Residual
1	Me	H	H	5.463	5.728	0.265
2	Et	H	H	5.097	5.741	0.644
3	H	H	H	4.699	5.751	1.052
4	Me	OMe	H	5.460	5.853	0.393
5	Me	Cl	H	5.602	5.847	0.245
6	Me	H	OMe	5.509	5.962	0.453
7	Me	H	Cl	5.648	5.750	0.102

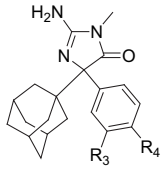

Compound	R_3	R_4	Observed	Predicted	Residual
8	H	H	5.815	5.940	0.124
[a] **9**	H	OEt	6.481	6.310	−0.172
10	H	O-n-Bu	6.06	6.446	0.386
11	H	OCF_3	6.328	6.267	−0.061
[a] **12**	Et	OMe	6.553	6.232	−0.321
[a] **13**	OMe	OMe	6.569	6.355	−0.214

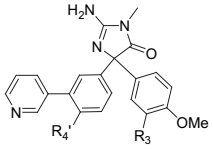

Compound	R_3	R_4'	Observed	Predicted	Residual
14	Me	H	7.398	7.383	−0.015
[a] **15**	OMe	H	7.046	7.356	0.310
16	OEt	H	7.301	7.003	−0.299
17	OPr	H	7.301	7.434	0.133
18	OBu	H	7.301	7.485	0.184
19	O-i-Pr	H	7.222	7.314	0.092
20	O-cyclopentyl	H	7.155	7.301	0.145
[a] **21**	cyclopentyl	H	6.921	6.858	−0.064
22	F	H	7.301	7.517	0.216
23	Cl	H	7.444	7.375	−0.069
24	CF_3	H	7.398	7.429	0.031
[a] **25**	CN	H	6.824	6.527	−0.297
[a] **26**	Me	Me	6.886	7.290	0.404

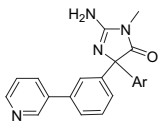

Compound	Ar	Observed	Predicted	Residual
[a] **27**		6.921	7.145	0.224
28		7.046	7.116	0.069

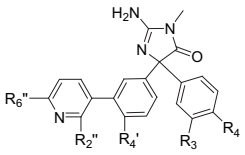

Compound	R3	R4	R4′	R2″	R6″	Observed	Predicted	Residual
29	Me	OMe	H	F	H	7.699	7.535	−0.164
30	Me	OMe	F	F	H	8.000	7.819	−0.181
31	H	OCF_3	H	F	H	7.222	7.309	0.087
32	H	OCF_3	H	H	OMe	6.046	6.611	0.565

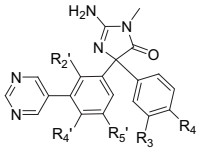

Compound	R_3	R_4	R_2'	R_4'	R_5'	Observed	Predicted	Residual
33	Me	OMe	H	H	H	7.523	7.341	−0.182
34	Me	OMe	H	F	H	7.699	7.656	−0.043
35	H	OCF_3	H	F	H	7.699	7.423	−0.276

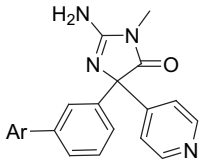

Compound	Ar	Observed	Predicted	Residual
36	H	5.572	5.966	0.394
37	Ph	6.886	7.186	0.300
38	3-MeOPh	7.523	7.257	−0.267
39	3-NCPh	7.398	7.410	0.012
40	3-FPh	7.301	7.394	0.093
41	2,3-diFPh	7.398	7.415	0.017
42	2,5-diFPh	7.699	7.049	−0.650
43	3,5-diFPh	7.222	7.147	−0.075
44	2-Pyrazinyl	7.155	7.174	0.019
45	3-Pyridinyl	7.222	7.294	0.072
46	2-Fluoropyrindin-3-yl	7.523	6.894	−0.630

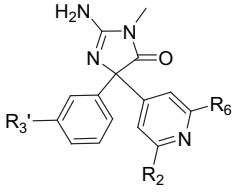

Compound	R_2	R_6	R_3'	Observed	Predicted	Residual
[a] **47**	Me	H	3-Pyridine	7.000	7.223	0.223
48	Me	H	5-Pyrimidine	7.097	7.339	0.242
49	Et	H	5-Pyrimidine	7.523	7.368	−0.156
50	*i*-Pr	H	5-Pyrimidine	7.155	7.388	0.232
[a] **51**	Me	Me	5-Pyrimidine	6.854	7.307	0.453
[a] **52**	Et	Me	5-Pyrimidine	6.824	7.335	0.511
53	Et	Et	5-Pyrimidine	7.523	7.331	−0.192
54	Et	Et	3- 2F-Pyridine	8	7.315	−0.685

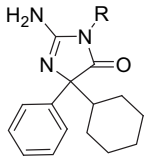

Compound	R	Observed	Predicted	Residual
55	Me	6.004	5.820	−0.185
56	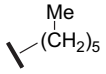	5.857	5.512	−0.346
57	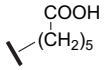	6.022	5.464	−0.558
58	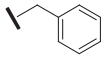	5.907	5.403	−0.505
59	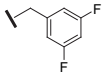	5.967	5.306	−0.661
60	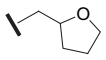	5.983	5.480	−0.503
61	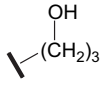	5.319	5.460	0.141

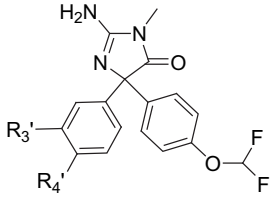

Compound	R_3'	R_4'	Observed	Predicted
[a] **62**		F	A*	7.128
[a] **63**		F	B*	6.616
[a] **64**		F	B	6.562
[a] **65**	NH_2	H	C*	5.880
[a] **66**	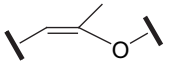		C	5.749
[a] **67**		H	B	6.935

Table 1 (*continued*)

Compound	R'_3	R'_4	Observed	Predicted
[a] **68**		H	B	6.567
[a] **69**	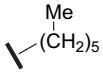	H	B	6.194

[a] test set; A≧7.0; B∈[6.0, 6.9], $C < 6.0$.

molecular architecture required for designing new specific non-peptide inhibitors of BACE-1 for the treatment of AD.

2. Results and discussion

In the present studies, SOMFA was employed for the analysis with the training set composed of 50 compounds whose biological activities are known to find out molecular features responsible for optimum biological activities. It should be noted that there are many factors affecting the outcome of a QSAR study. As for 3D-QSAR method, molecular alignments and charge-assigning methods are the most important factors, while grid spacing is not sensitive for SOMFA according to the previous report [18–20]. Hence, in our research, four alignments and two charge-assigning methods (Gasteiger–Huckel charges and AM1) with grid spacing of 1.0 Å were investigated to produce eight SOMFA models. The superposition of the aminohydantoin compounds derived from the four different alignment modes was depicted in Fig. 2. Model **A1** and **A2** correspond to the optimization of structures by MM2 and AM1 method followed by alignment according to the common aminohydantoin group (***a*** alignment method). From the Fig. 2, it was shown that the conformations of 5, 5-disubstituted aryl groups derived from the ***a*** alignment are very inconsistent, so the dihedrals of C2-C3-C12-C17, C2-C3-C5-C10 and C17-C16-C18-C19 were changed to 65.7°, 30.1° and 51.4° respectively according to the X-ray structure of BACE1-**35** complex (pdb code: 3INH) to produce the ***b*** alignment. Model **C1** and **C2** correspond to the superposition of docked conformations (***c*** alignment method), while model **D1** and **D2** correspond to the further alignment of the docked conformations according to the common aminohydantoin scaffold (***d*** alignment method).

To obtain the active conformations of 5, 5-disubstituted aminohydantoins, a series of docking experiments were conducted. To validate our docking protocol, compound **35** was redocked to active site of the BACE-1 protein and the RMSD with the X-ray structure is only 0.9 Å (Fig. 3). Firstly, the crucial hydrogen bond interactions of aminohydantoin group with Asp94, Asp290 were identified. Moreover, the H-bond of 4-OCF_3 with Trp138 were also recognized. The only difference between the docking and X-ray conformation resides in the angle of two planes defined by the pyrimidine ring and its vicinal aryl group. The angle of docked structure is 73.7°, which is greater than that of X-ray structure by 22.3°. It can be ascribed to the crystal waters, which play an essential role in the formation of the ligand–enzyme complex. For example, WAT-3 serves as a water bridge to link the 4′-F and Phe170. In addition, as for the X-ray structure, the 5-pyrimidine formed the hydrogen bond with WAT-2 which further interacts with Ser291, while for docked one, the nitrogen of 5-pyrimidine group tends to form the hydrogen bond with WAT-1 which forms the hydrogen bonds with the Gly73 and Thr294.

For SOMFA model A1～D1, Gasteiger–Huckel charges were added to the compounds, however, all the electrostatic potential

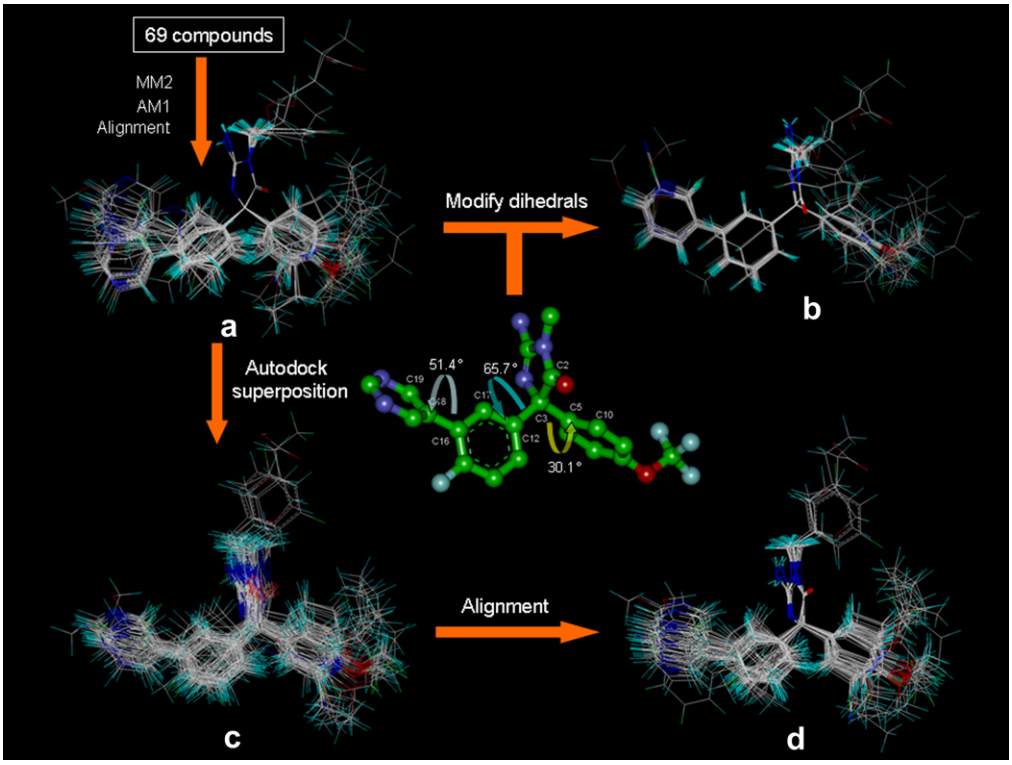

Fig. 2. Four alignment modes: *a*: the optimization of structures by MM2 and AM1 method followed by alignment according to the common aminohydatoin group, *b*: Modification of the three dihedrals of the *a* alignment compounds according to the X-ray structure of compound **35**. *c*: the superposition of docked conformations. *d*: the alignment of the docked conformations according to the common aminohydatoin scaffold.

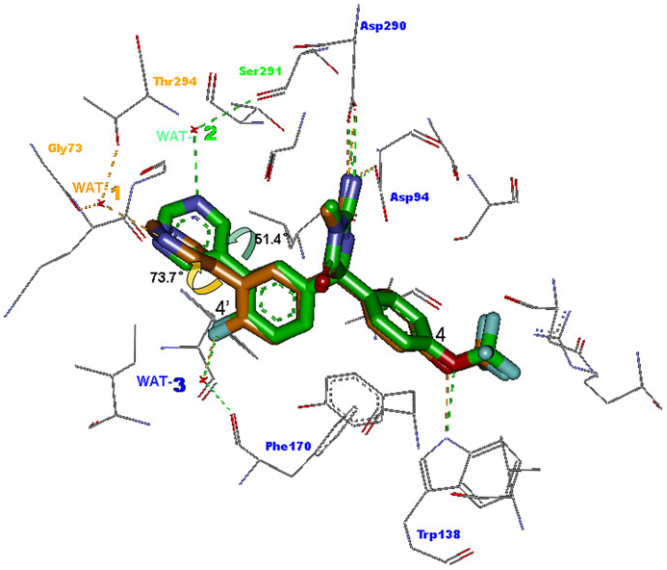

Fig. 3. The superposition of compound **35** derived from X-ray structure (green) and docked conformation (orange).

contribution c_2 is zero, indicating that the accuracy of the charge method is not suitable for this system (Table 2). As far as the alignment method was concerned, as we expected, the model derived from the ***b*** method is superior to ***a***, indicating that if the active ligand conformation was available, construction of other derivatives by using the ligand as template is more appropriate. Although the non-cross-validated correlation coefficient (r^2) of **B1** is higher than that of **A1** by about 0.04, the r^2 of **B1** model was lower than that of **C1** by 0.03. So if the three-dimensional structure of target protein is available, superposition of docked conformation is better than the above two alignment methods. Beyond our predictions, instead of improving the predict activity, further alignment of the docked conformation by the common amino-hydantoin moiety slightly degenerates the SOMFA model. It can be attributed to the different substituent groups which may lead to the tiny movement of the aminohydantoin scaffold.

Furthermore, as for A2∼D2, AM1 charges were used and the qualities of all the SOMFA models were improved apparently. The r^2 of model **C2** reached to 0.842, the highest one of all the eight SOMFA models. (Table 2)

The observed and predicted activities of the training set are reported in Table 1 using the best Model **C2**. Fig. 4a showed a satisfied linear correlation.

It's well known that the best way to validate a 3D-QSAR model is to predict biological activities for some compounds of test set. The

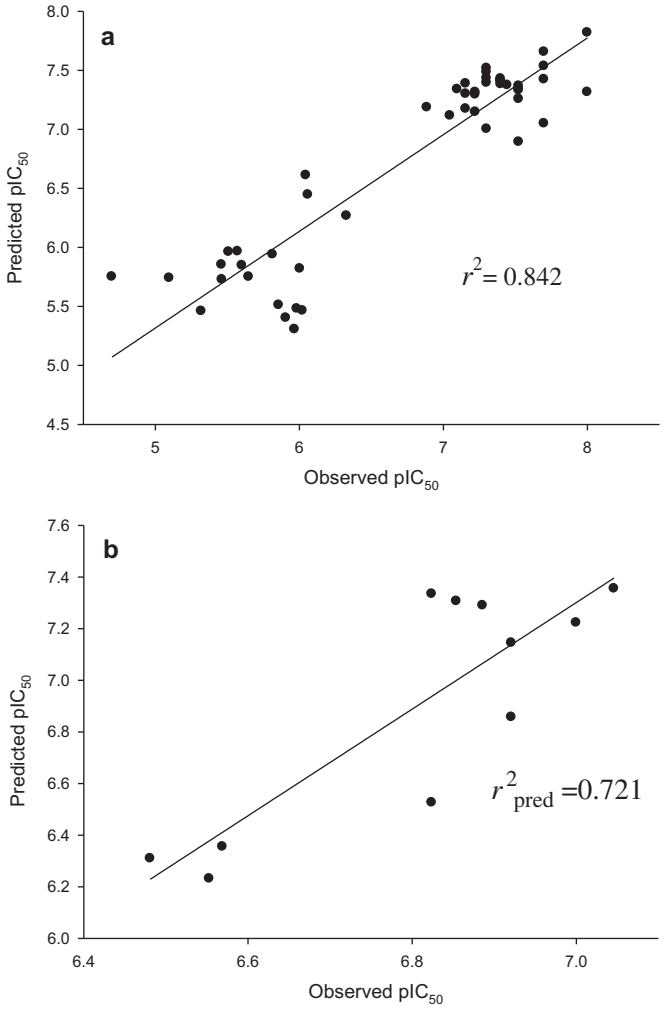

Fig. 4. Predicted versus observed pIC_{50} in the *a*: training set; *b*: test set.

SOMFA analysis of the test set composed of 11 compounds is reported in Table 1. Most of the compounds in test set show good correlation ($r^2_{pred} = 0.721$) between observed and predicted values (Fig. 4b). To further test the application scope of the SOMFA model, a variety of 3′-substituted aminohydantoin derivatives (compound **62∼69** in Table 1) were docked and the predicted activity were in good agreement with the reference. It should be noted that although r^2 of model **D2** is very close to **C2**, the predictive ability r^2_{pred} of **D2** model is 0.633, which is lower than that of **C2** by 0.088.

Table 2
Statistics of the various SOMFA models.

Model	Alignment	Charge	r^2	s	F	c_1	c_2	q^2
A1	*a*	Gasteiger	0.753	0.39	146.26	1.0	0.0	0.636
B1	*b*	Gasteiger	0.792	0.36	183.56	1.0	0.0	0.758
C1	*c*	Gasteiger	0.822	0.34	222.14	1.0	0.0	0.780
D1	*d*	Gasteiger	0.817	0.34	214.63	1.0	0.0	0.771
A2	*a*	AM1	0.768	0.36	159.67	0.6	0.4	0.640
B2	*b*	AM1	0.799	0.35	191.34	0.7	0.3	0.759
C2	***c***	**AM1**	**0.842**	**0.31**	**254.75**	**0.5**	**0.5**	**0.792**
D2	*d*	AM1	0.841	0.31	254.04	0.5	0.5	0.791

r^2, non-cross-validated correlation coefficient; *s*, standard error of estimate; *F*, F-test value; c_1, mixing coefficient of SOMFA model, representing the shape potential contribution; $c_2 = 1 - c_1$, representing the electrostatic potential contribution; q^2, cross-validated correlation coefficient.

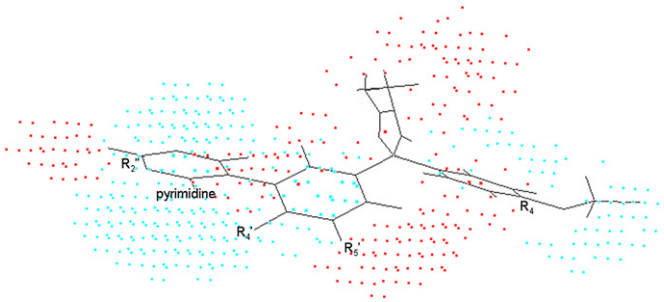

Fig. 5. The electrostatic potential master grid with compound **35**. Red represents areas where positive potential is favorable, or negative charge is unfavorable. Blue represents areas where negative potential is favorable, or positive charge is unfavorable.

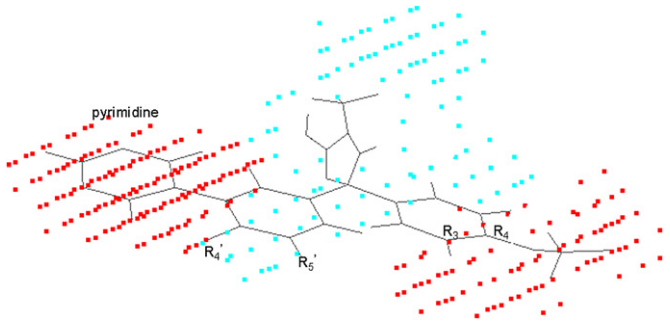

Fig. 6. The shape potential master grid with compound **35**. Red represents areas of favorable steric interaction. Blue represents areas of unfavorable steric interaction.

SOMFA calculation for both shape and electrostatic potentials are performed then combined to get an optimal coefficient $c_1 = 0.5$ according to eq (1). The visualization of the electrostatic potential master grid and shape master grid of the best SOMFA model is showed in Figs. 5 and 6, respectively, with the active compound **35** as the reference. Each master grid map is colored in two different colors for favorable and unfavorable effects. That is, the electrostatic features are red (more positive charge increases activity, or more negative charge decreases activity) and blue (more negative charge increases activity, or more positive charge decreases activity), and the shape feature are red (more steric bulk increases activity) and blue (more steric bulk decreases activity), respectively.

SOMFA analysis result indicates the electrostatic contribution is equal to shape ($c_1 = 0.5$). The SOMFA electrostatic potential for the analysis is presented as master grid in Fig. 5. In this map of important features, we find a high density of blue points around the substituent R4, R4′ and pyrimidine ring, which means some electronegative groups are favorable. We also find a high density of red points around the R5′, R2″ of pyrimidine ring and aminohydantoin group which means some strong electropositive groups are favorable.

Meanwhile, in the map of shape master grid in Fig. 6, we can find a high density of red points around the R3, R4 and pyrimidine ring, which means a favorable steric interaction; simultaneously, we find a high density of blue points around the R4′, R5′ and aminohydantoin group, which means an unfavorable steric interaction may be expected to enhance activities.

3. Conclusion

A predictive SOMFA 3D-QSAR model for 5, 5-disubstituted aminohydantoin derivatives having wide variations in structure and potency profile against BACE-1 has been developed. To get a best SOMFA model, superposition of docked conformation is needed. The master grid obtained for the SOMFA models indicated electrostatic and shape potential contributions can be mapped back onto structural features relating to the trends in activities of the molecules, which will be helpful in designing novel molecules with improved spectrum of activity. It should be mentioned that the compound class suffers from PGP-transportion which may limit the value for further development. May be a SOMFA analysis of BACE inhibition and PGP transportion may provide a rational guidance for future improvements.

4. Experimental section

4.1. Data set

A dataset of 69 molecules, belonging to 5, 5-disubstituted aminohydantoin derivatives as human BACE-1 inhibitors and showing wide variations in their structure and potency profiles, were taken from the literature and used for SOMFA study [9]. Eight different models were generated for this series using a training set of 50 molecules. Predictive powers of the resulting models were evaluated by a test set of 19 molecules with uniformly distributed biological activities. The general structures of the training and test set molecules have been presented in Table 1.

4.2. Biological activities

The negative logarithm of the measured IC_{50} (M) against human BACE-1 enzyme as pIC_{50} was used as dependent variable [21], thus correlates the data linear to the free energy change.

4.3. Molecular docking

AutoDock version 4.0 [22] was used for the docking simulation. Lamarckian genetic algorithm (LGA) was selected for ligand conformational searching because it adds local minimization to the genetic algorithm, enabling modification of the gene population. For each compound, the docking parameters were as follows: trials of 100 dockings, population size of 150, 10 million energy evaluations. Other parameters are default. BACE-1 X-ray structure was retrieved from RCSB (pdb code 3INH). The jobs were distributed to the Lenovo Think station S20 in Redhat WS4.0 linux. Final docked conformations were clustered by use of a tolerance of 1.5 Å root-mean-square deviations (RMSD). The top energy conformations were used to superposition for the further SOMFA analysis.

4.4. Molecular modeling and alignment

The three-dimensional structures of the 5, 5-disubstituted aminohydantoins were constructed with the Discovery Studio 2.1 running on an Intel Centrino2 1.83 GHz Processor/Microsoft Win 7 Home Edition platform and were subjected to energy minimization using molecular mechanics (MM2). The minimization is continued until the root mean square (RMS) gradient value reaches a value smaller than 0.001 kcal/mol Å. The Hamiltonian approximations Austin model 1 (AM1) method available in the MOPAC2009 [23] is adopted for re-optimization until the root mean square (RMS) gradient attains a value smaller than 0.001 kcal/mol Å. Unless otherwise indicated, all parameters were kept default. The alignment includes the following methods: (***a***) alignment of structures optimized by MM2 and AM1 method according to the common aminohydantoin group, (***b***) further modification of the three dihedrals of ***a*** alignment compounds according to the X-ray structure of BACE1-compound **35** complex (pdb code: 3INH) (***c***) superposition of docked conformations (***d***) Further alignment of the docked conformations according to the common aminohydantoin scaffold.

4.5. SOMFA 3D-QSAR models

In the SOMFA study, a 40 × 40 × 40 Å grid originating at (−20, −20, −20) with a resolution of 1 Å, was generated around the aligned compounds. Eight different models using different alignments and charge method have been presented in Table 2. For all of the studies, electrostatic and shape potential are developed. In order to combine the predictive power of these two properties into one final model, we sum up their individual predictions using a weighted average of the shape and electrostatic potential based QSAR, using a mixing coefficient (c_1) as illustrated in eq (1).

$$\text{Activity} = c_1\,\text{Activity}_{\text{shape}} + (1 - c_1)\,\text{Activity}_{\text{ESP}} \quad (1)$$

The partial least square (PLS) algorithm was in conjugation with leave one out (LOO) cross-validation which was used to develop the final model. The predictive ability of the model is quantitated in terms of q^2 which is defined in eq (2).

$$q^2 = (\mathrm{SD} - \mathrm{PRESS})/\mathrm{SD} \quad (2)$$

where $\mathrm{PRESS} = \sum(Y_{pred} - Y_{mean})^2$ and $\mathrm{SD} = \sum(Y_{actual} - Y_{mean})^2$

SD is the sum of squares of derivations of the observed values from their mean and PRESS is the prediction error sum of squares.

The q^2 can take up values in the range from 1, suggesting a perfect model, to less than 0 where errors of prediction are greater than the error from assigning each compound mean activity of the model.

Because the final equations are not very useful to represent efficiently the SOMFA models, 3D master grid maps of the best models are displayed by Grid-Visualizer program. These grids represent area in space where steric and electrostatic field interactions are responsible for the observed variations of the biological activity.

Acknowledgment

The authors are grateful to the support of the National Science Foundation of China (30901743), the State Key Laboratory of Drug Research and Doctoral Fund of Ministry of Education.

References

[1] L.A. Thompson, J.J. Bronson, F.C. Zusi, Curr. Pharm. Des. 11 (2005) 3383–3404.
[2] a) G.G. Glenner, C.W. Wong, Biochem. Biophys. Res. Commun. 120 (1984) 885–890;
b) M. Goedert, C.M. Wischik, R.A. Crowther, J.E. Walker, A. Klug, Proc. Natl. Acd. Sci. U S A 85 (1988) 4051–4055.
[3] J. Tang, X. He, X. Huang, L. Hong, Curr. Alzheimer Res. 2 (2005) 261–264.
[4] Y. Luo, B. Bolon, S. Kahn, B.D. Bennett, S. Babu-Khan, P. Denis, W. Fan, H. Kha, J. Zhang, Y. Gong, L. Martin, J.C. Louis, Q. Yan, W.G. Richards, M. Citron, R. Vassar, Nat. Neurosci. 4 (2001) 231–232.
[5] X. Lin, G. Koelsch, S. Wu, D. Downs, A. Dashti, J. Tang, Proc. Natl. Acad. Sci. U S A 97 (2000) 1456–1460.
[6] W.H. Huang, R. Sheng, Y.Z. Hu, Curr. Med. Chem. 16 (2009) 1806–1820.
[7] R. Silvestri, Med. Res. Rev. 29 (2009) 295–338.
[8] C.A. Coburn, S.J. Stachel, Y.M. Li, D.M. Rush, T.G. Steele, D.E. Chen, M.K. Holloway, M. Xu, Q. Huang, M.T. Lai, J. DiMuzio, M.C. Crouthamel, X.P. Shi, V. Sardana, Z. Chen, S. Munshi, L. Kuo, G.M. Makara, D.A. Annis, P.K. Tadikonda, H.M. Nash, J.P. Vacca, T. Wang, J. Med. Chem. 47 (2004) 6117–6119.
[9] a) M.S. Malamas, J. Erdei, W.G. Wan, J. Turner, Y. Hu, E. Wagner, K. Fan, R. Chopra, A. Olland, J. Bard, S. Jacobsen, R.L. Magolda, M. Pangalos, A.J. Robichaud, J. Med. Chem. 53 (2010) 1146–1158;
b) M.S. Malamas, K. Barnes, M. Johnson, Y. Hui, P. Zhou, J. Turner, Y. Hu, E. Wagner, K. Fan, R. Chopra, A. Olland, J. Bard, M. Pangalos, Bioorg. Med. Chem. 18 (2010) 630–639;
c) P. Zhou, Y. Li, Y. Fan, Z. Wang, R. Chopra, A. Olland, Y. Hu, R.L. Magolda, M. Pangalos, P.H. Reinhart, M.J. Turner, J. Bard, M.S. Malamas, A.J. Robichaud, Bioorg. Med. Chem. Lett. 20 (2010) 2326–2329;
d) M.S. Malamas, J. Erdei, I. Gunawan, K. Barnes, M. Johnson, Y. Hui, E. Wagner, K. Fan, A. Olland, J. Bard, A.J. Robichaud, J. Med. Chem. 52 (2009) 6314–6323;
e) M.S. Malamas, A.J. Robichaud, A.M. Porte, K.M. Morris, W.R. Solvibile, J. Kim, WO 2008118379 A2 20081002, PCT Int. Appl. (2008).
[10] A.K. Ghosh, C.F Liu, T. Devasamudram, H. Lei, L.M. Swanson, S.V. Ankala, J.C. Lilly, G.M. Bilcer, WO 2009015369 A2 20090129, PCT Int. Appl. (2009).
[11] A.C. Cralg, S.E. Amy, J.S. Shawn, B.O. David, J.H. Darla, M.K. Holloway, WO 2005097767 A1 20051020, PCT Int. Appl. (2005).
[12] M. S. Malamas,; W. F. Fobare, W.R.S. JR, F.E. Lovering, J.S. Condon, A.J. Robichaud, US20060173049 (2006).
[13] B. Ellen, B. Robert, C.J. Alfonzo, R. Allen, H.R. Charies, S. Malcolm, S. Mark, D. Winter, H.L. Jos, WO 2006017844 A1 20060216, PCT Int. Appl. (2006).
[14] D.C. Cole, E.S. Manas, J.R. Stock, J.S. Condon, L.D. Jennings, A. Aulabaugh, R. Chopra, R. Cowling, J.W. Ellingboe, K.Y. Fan, B.L. Harrison, Y. Hu, S. Jacobsen, G. Jin, L. Lin, F.E. Lovering, M.S. Malamas, M.L. Stahl, J. Strand, M.N. Sukhdeo, E. Wagner, J. Wu, P. Zhou, J. Bard, J. Med. Chem. 49 (2006) 6158–6161.
[15] R.B. Govinda, O.S. Jeffrey, A.M. Mark, A.L. Christopher, D.B. Shawn, H.C. Joe, D.D. David, WO 02088101 A2 20021107, PCT Int. Appl. (2002).
[16] D.D. Robinson, P.J. Winn, P.D. Lyne, W.G. Richards, J. Med. Chem. 42 (1999) 573–583.
[17] R.D. Cramer, D.E. Patteerson, J.D. Bunce, J. Am. Chem. Soc. 110 (1988) 5959–5967.
[18] M.Y. Li, L.P. Du, B. Wu, L. Xia, Bioorg. Med. Chem. 11 (2003) 3945–3951.
[19] S. Thareja, S. Aggarwal, T.R. Bhardwaj, M. Kumar, Europ. J. Med. Chem. 44 (2009) 4920–4925.
[20] S. Aggarwal, S. Thareja, T.R. Bhardwaj, M. Kumar, Steroids 75 (2010) 411–418.
[21] N. Sachan, S.S. Kadam, V.M. Kulkarni, J. Enzym. Inhib. Med. Chem. 22 (2007) 267–276.
[22] G.M. Morris, R. Huey, W. Lindstrom, M.F. Sanner, R.K. Belew, D.S. Goodsell, A.J. Olson, J. Comput. Chem. 30 (2009) 2785–2791.
[23] J.P.S. James, Stewart Computational Chemistry. Colorado Springs, CO, USA, 2008.http://OpenMOPAC.net.